Numerical Approaches to Simulating Nonlinear Ultrasound Fields Generated by Diagnostic-Type Transducers

M. M. Karzova*, P. V. Yuldashev, P. B. Rosnitskiy, and V. A. Khokhlova

Faculty of Physics, Moscow State University, Moscow, 119991 Russia
**e-mail: masha@acs366.phys.msu.ru*

Abstract—Two theoretical approaches for simulating nonlinear focused ultrasound fields generated by a diagnostic convex array are compared. The first model is based on the three-dimensional Westervelt equation and describes the full structure of the array field with high accuracy. However, it requires great computational resources and is technically difficult. The second model is based on an axially symmetric form of the parabolic KZK equation for estimating the strength of nonlinear effects in the focal region of a beam, which reduces the computational time by a factor of several hundreds. To establish the boundary conditions to the KZK model, the radius and the focal length of a circular piston source are defined such that the simulated field on the beam axis in the linear case fits the real structure of the field in the focal region. It is shown that the parabolic model can be used to accurately describe the spatial and temporal structure of the field generated by a diagnostic transducer in the focal region of the beam along its axis and in the plane of the beam's electronic focusing.

INTRODUCTION

In modern diagnostic and therapeutic medical applications of ultrasound, technologies that employ acoustic radiation force of an ultrasound beam to affect solid concrements or biological tissues have begun developing rapidly [1–4]. One example of this is the new technology for moving small stones out of kidneys [1, 2]. The acoustic radiation force is also used in innovative ultrasound imaging techniques for generating shear waves in biological tissue, and for shifting tissue to observe its relaxation [3, 4]. Under clinical conditions, this force impact can be induced by conventional diagnostic transducers that function in the long-pulse mode with increased intensity, compared to the standard imaging modes [1, 2]. In this work, we compare two theoretical models for describing nonlinear focused ultrasound fields generated by a typical diagnostic transducer in the form of a convex array.

THEORETICAL MODELS

We use two theoretical models to determine the parameters of the spatial and temporal structure of a nonlinear focused ultrasound field generated by a diagnostic transducer when it is calibrated in water. The first model is based on the Westervelt equation, which is written in the moving coordinate system [5]:

$$\frac{\partial^2 p}{\partial \tau \partial z} = \frac{c_0}{2} \Delta p + \frac{\beta}{2\rho_0 c_0^3} \frac{\partial^2 p^2}{\partial \tau^2} + \frac{\delta}{2 c_0^3} \frac{\partial^3 p}{\partial \tau^3}. \qquad (1)$$

Here, p is the acoustic pressure; z is the direction along the beam axis; $\tau = t - z/c_0$, where t is time; $\Delta p = \partial^2 p/\partial z^2 + \partial^2 p/\partial y^2 + \partial^2 p/\partial x^2$; x and y are spatial coordinates that are transverse to z; and ρ_0, c_0, β, and δ are density, speed of sound, nonlinearity, and the thermoviscous absorption in the medium, respectively. The physical parameters in Eq. (1) that correspond to propagation in water are $\rho_0 = 998$ kg m^{-3}; $c_0 = 1486$ m s^{-1}; $\beta = 3.5$; $\delta = 4.33 \times 10^{-6}$ m^2 s^{-1}. Equation (1) considers nonlinear diffraction effects and thermoviscous absorption.

The numerical algorithm for simulating Eq. (1) was based on the second-order operator splitting and used a combined time-frequency approach to describe different physical effects at each step of the numerical grid along the beam axis [6]. The diffraction operator is calculated with respect to the frequency-domain representation for each of the harmonics using the analytical solution for an angular spectrum. Two algorithms were used to calculate the nonlinear operator: at short distances from the source, computations were performed in the frequency-domain representation according to the fourth-order Runge–Kutta method. When the amplitude of the tenth harmonic starts to exceed 1% of the fundamental frequency amplitude, they were performed in the time-domain representation using a conservative Godunov-type scheme [7]. Absorption was calculated using exact analytical solutions for each of the harmonics. The parameters of the numerical schemes were chosen as follows: the step
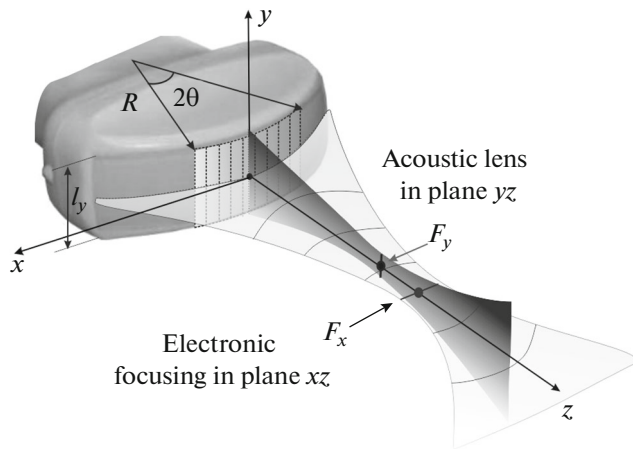
Fig. 1. Geometry of a diagnostic ultrasound transducer in the form of a convex array.

along the beam axis $dz = 0.075$ mm; the steps along the transverse coordinates $dx = dy = 0.02$ mm; and the maximum number of harmonics was 750.

The second model used simplifying assumptions regarding the parabolic approximation with allowance for diffraction effects and the axial symmetry of the beam. A nonlinear ultrasound beam in this case was described by the Khokhlov−Zabolotskaya−Kuznetsov (KZK) equation [8]

$$\frac{\partial^2 p}{\partial \tau \partial z} = \frac{1}{r}\frac{\partial}{\partial r}\left(r\frac{\partial p}{\partial r}\right) + \frac{\beta}{2\rho_0 c_0^3}\frac{\partial^2 p^2}{\partial \tau^2} + \frac{\delta}{2c_0^3}\frac{\partial^3 p}{\partial \tau^3}, \quad (2)$$

where r is the radial coordinate.

Numerical simulations of Eq. (2) also used operator splitting procedure. The diffraction operator was calculated with respect to the spectral representation using an implicit scheme at distances of up to 10% of the focal depth, and then at greater distances using the Crank−Nicolson method. To allow for dissipative and nonlinear effects, we used the same numerical algorithms as in solving the Westervelt equation (1). The step along the radial coordinate in our numerical computations was 0.0025 mm, the step with respect to coordinate z along the beam axis was 0.02 mm, and the wave spectrum was up to 1000 harmonics. The algorithm was adapted for parallel computing using the OpenMP software, which enabled us to shorten the calculation time to several tens of minutes, while the simulation of the three-dimensional Westervelt equation (1) took several days.

SETTING BOUNDARY CONDITIONS

The boundary condition in simulating Westervelt equation (1) corresponded to the parameters of the standard diagnostic ultrasound transducer whose geometry is given in Fig. 1 (a Philips C5-2 convex array). The emitting surface of the transducer was a

region of the cylindrical surface with height l_y. Its surface contained 128 array elements, varying the phase of which could focus the beam in the xz plane to depth F_x. The signal can be radiated in the mode of feeding a different number of the central elements of the array. In this work, we consider a clinically important case of feeding 40 active elements of the array, which was used in pilot experiments on repositioning kidney stones, and a case of using the entire surface of the array (128 elements). For an ultrasound beam not to diverge in the plane yz, the transducer has an embedded acoustic lens that focuses the field to depth F_y.

The geometrical parameters of the transducer were determined earlier by fitting the boundary conditions while calculating the Rayleigh integral so that the results from computing the linear field along axis z of the transducer and in the focal plane were in the best agreement with the results from measurements using a hydrophone [9]. Focal depth F_x for the electronic focusing of the transducer was 50 mm. The surface's radius of curvature was $R = 38$ mm; its height was $l_y = 12.5$ mm; angular size θ of one element was 5.2×10^{-2} rad; and focal depth F_y for focusing by the acoustic lens was 86 mm for 40 elements and 70 mm for 128 active elements of the array. The initial condition in our simulation was a periodic wave with frequency $f = 2.3$ MHz and uniform distribution of the amplitude along the surface. Focal depth $F_x = 50$ mm was ensured by a delay of the wave phase along cylindrical coordinate θ according to $2\pi f\left(\sqrt{(R\sin\theta)^2 + (R - R\cos\theta + F_x)^2} - F_x\right)/c_0$. Calibration (which had been done earlier) revealed that the voltage of 1 V applied to the array corresponded to the amplitude of an ultrasound wave of 24.0 kPa when feeding 40 elements of the array, and an amplitude of 18.8 kPa when using all 128 elements. At higher voltages, the increase in the amplitude of the pressure at the radiator was proportional to the voltage [9].

To set the boundary conditions when simulating KZK equation (2), it was necessary to determine radius r_0 of the circular piston source and its focal length F. In [10], it was shown that the structure of the acoustic field during focusing was mainly determined by the ratio of these quantities, r_0/F. Parameters r_0 and F of the parabolic model were chosen such to ensure the minimum difference between the distributions of the pressure amplitude in the focal peak along axis z that were obtained for linear ($\beta = 0$) parabolic (2) and full three-dimensional diffraction models (1). For 40 active elements of the array, the parameters of the circular equivalent radiator were $r_0 = 1.2$ cm and $F = 7.0$ cm; for 128 elements, they were $r_0 = 2.4$ cm and $F = 5.9$ cm.

The parabolic approximation when describing the diffraction effects in KZK equation (2) initially restricted its applicability to small focal angles [11].

However, it was shown in [12−15] that a certain way of setting the boundary conditions allowed KZK equation (2) to also describe with high accuracy strongly focused fields, along with fields that did not have full axial symmetry as, e.g., in the case of multielement radiators for noninvasive ultrasound surgery [16, 17]. The main goal of this work was to test the applicability and accuracy of simple and fast numerical calculations that use KZK equation (2) to describe strongly focused nonlinear fields with complex geometry, where there is no axial symmetry and the condition that focal angles be small is not met. The model of a diagnostic transducer with the feeding of a different number of elements was the one most illustrative for this purpose and most important for practical applications.

RESULTS AND DISCUSSION

The distribution of the pressure amplitude along axis z of the diagnostic transducer, calculated for the linear propagation of a wave using the full three-dimensional diffraction model and the parabolic approximation, is given in Fig. 2. It is clearly seen that the parabolic model (dotted curve) satisfactorily describes the structure of the field near the focal peak, but diverges from the three-dimensional model (solid curve) in the oscillatory region of the near field of the array (Figs. 2a, 2b) and for the case of feeding 128 elements in the region behind the focus (Fig. 2b). At the same time, for the configuration of 40 active elements of the array, the parabolic model predicts a higher amplitude of the oscillating pressure of the near field than the full diffraction model. In contrast, when all 128 elements of the array are fed into the parabolic model, the amplitude of the pressure of the near field is underestimated.

The good agreement between the results from linear calculations in the region of the focal peak allowed us to suggest that the parabolic model would also correctly describe the structure of the field of the beam near the focus in the case of nonlinear wave propagation. However, it should be noted that the initial discrepancy between the results of the two models in the structure of the near field in the linear case would be important when considering nonlinear effects. We suggest that overestimating the amplitude of the near field in the parabolic model would enhance the nonlinear effects along the path of the wave propagation to the focus. Before the shock is formed [10], it would be expressed as a stronger increase in the peak positive pressure in the wave profile at the focus for the parabolic model, as compared to the three-dimensional model [10, 18]. Once the shock was formed, nonlinear energy absorption at the shock front would play an important role, and it would be difficult to predict the qualitative difference between the results obtained using the parabolic and three-dimensional models.

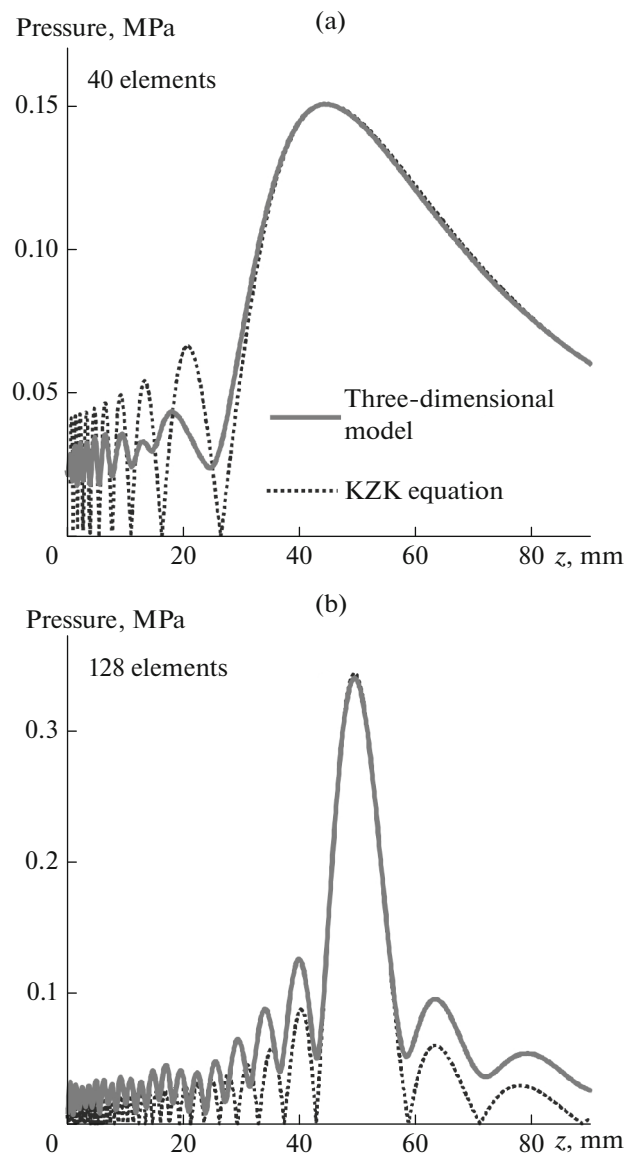We tested the applicability of the KZK equation and assessed its accuracy for describing the temporal

Fig. 2. Distribution of the amplitude of the pressure of an ultrasound field on the z axis of a radiator with linear propagation at a voltage of 1 V (a) for 40 active elements of the array and (b) for 128 elements.

and spatial structure of the nonlinear focused field of our diagnostic array. Figure 3 gives the results from simulations for the feeding of 40 active elements of the array at a voltage of 25 V. The peak positive and peak negative pressures in the wave profile at the focus in this case differ greatly (Figs. 3a, 3b), and the wave profile according to the definition in [10] contains a developed shock (Fig. 3c); i.e., the shock front starts at zero pressure level. It can be seen from the figure that the parabolic model satsifactorily describes the distribution of the peak negative pressure in the focal region on the beam axis (Fig. 3a) and in the focal region along direction x of the arrangement of the array elements (Fig. 3b). The peak positive pressure at the beam axis
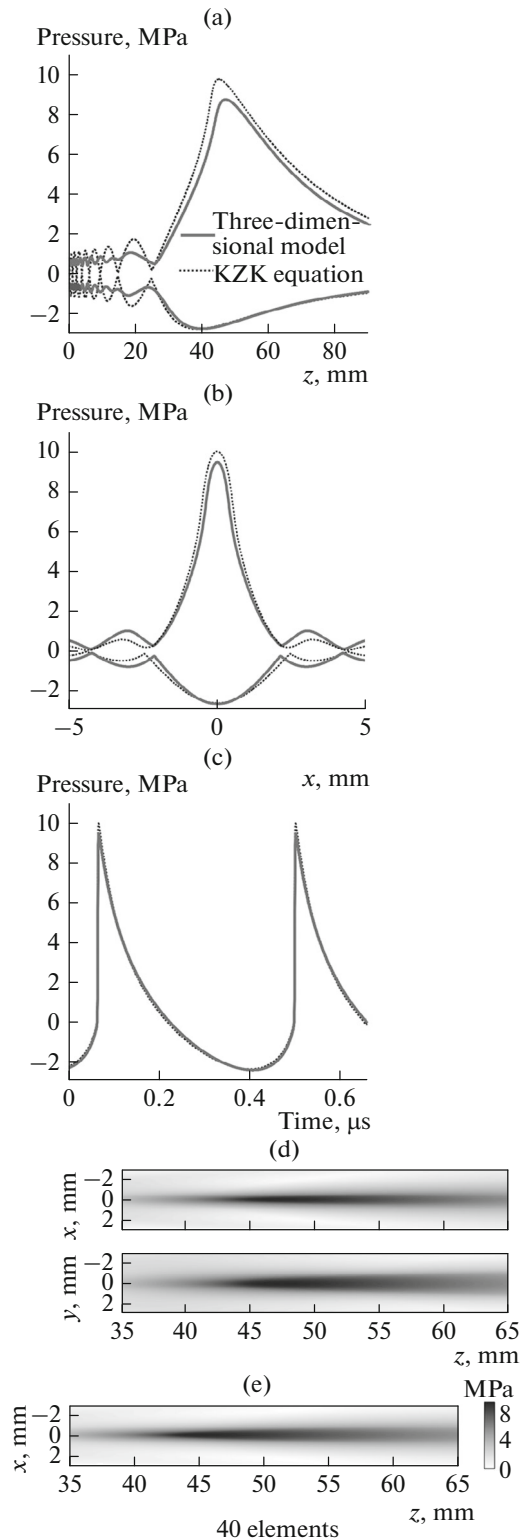
Fig. 3. Comparison of the results from simulating a nonlinear ultrasound field irradiated by 40 active elements of a diagnostic array at a voltage of 25 V. The distribution of the peak positive and peak negative pressures (a) on the z axis and (b) in transverse direction x in the focal plane $z = 50$ mm; (c) wave profiles at the focus; and two-dimensional distributions of the peak positive pressure, calculated using (d) the three-dimensional Westervelt equation and (e) axially symmetric parabolic model.

z was overestimated by as much as 15% in the region of the focal peak, but it correctly describes the qualitative structure of the distribution (Fig. 3a). It is interesting that, despite the great simplification of the axially symmetric parabolic model, the wave profile predicted by it corresponds at the focus ($z = 50$ mm) to the profile calculated using the Westervelt equation, with an accuracy of up to 5% (Fig. 3c).

The axial symmetry of the parabolic model did not allow us to obtain quantitative information on the structure of the field in focal plane yz of the acoustic lens. In this plane, the diagnostic transducer is weakly focused, and the field structure on the beam axis is determined mainly by the stronger electronic focusing in plane xz. It can be seen from Figs. 3d and 3e that the two-dimensional spatial structure of the peak positive pressure computed using the parabolic model is in good agreement with the similar distribution in focal plane xz of electronic focusing that was obtained in the three-dimensional model. When using 40 elements of the array, the size of the active surface of the transducer in directions x and y differs by only 10%, so the distributions of the peak pressures in focal planes xz and yz are similar in the structure and dimensions of the focal region (Fig. 3d).

We now consider an asymmetric case of feeding all 128 elements of the diagnostic array (Fig. 4). For this configuration, the KZK equation predicts the formation of a developed shock in the focal wave profile at a voltage of 40 V (Fig. 4c), while it actually formed at 22 V. This corresponds to the above situation where the difference between the structures of the near field calculated by both models in the linear case does not clearly answer what would be the qualitative difference in the structure of the nonlinear fields after formation of the developed shock. Our simulation results showed that the distribution of the peak positive and negative pressures on the transducer axis (Fig. 4a) and in the focal plane (Fig. 4b) are adequately described by the KZK equation, with the value of the peak positive pressure in the focus being predicted with an error of 3% and the value of the pressure jump at the shock front being predicted with an error of 18% (Fig. 4c). The two-dimensional spatial distributions of the peak pressures for 128 elements differ greatly in planes xz and yz (Fig. 4d). Though the spatial structure of the peak positive pressure obtained using the parabolic model is closer to the real distribution in plane xz than in plane yz, the size of the focal region in directions x and z was found to be wider.

The KZK equation may thus be considered suitable for estimating the parameters of the nonlinear ultrasound field of a diagnostic transducer in the focal region on the beam axis and in the plane of electronic focusing with an approximate error of 15% in the case of the formation of a developed shock in the wave profile at the radiator focus.
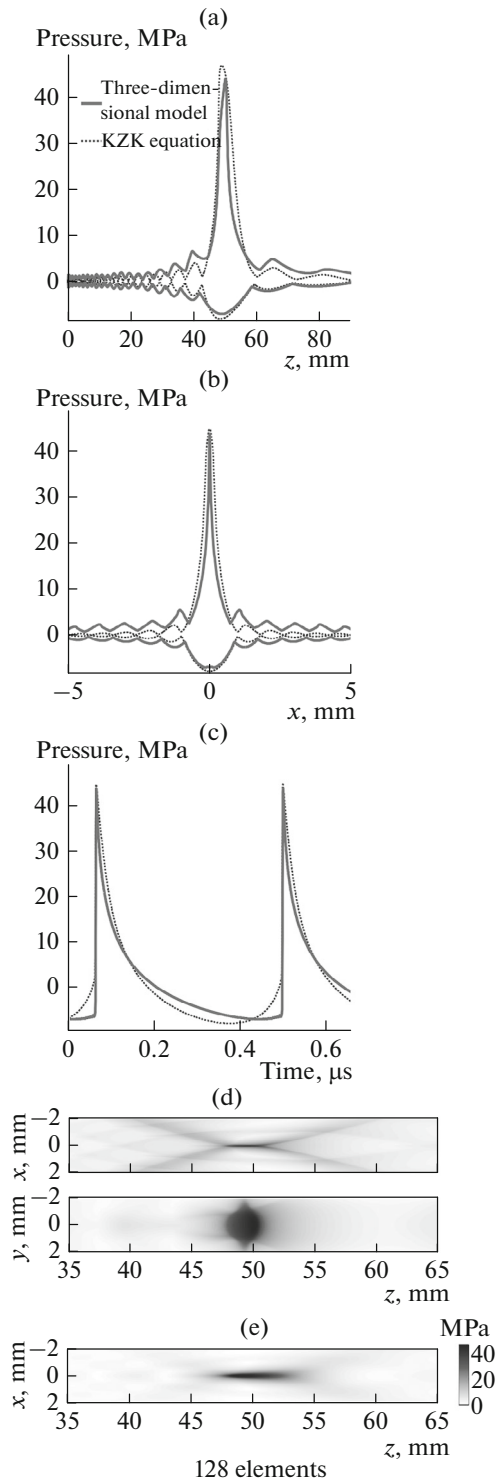
Fig. 4. Results from simulating the nonlinear field of a diagnostic transducer when feeding all 128 elements of an array at a voltage of 40 V. The figure's structure is similar to that of Fig. 3.

used in numerical simulations to estimate the parameters of the spatial and temporal structure of a nonlinear ultrasound filed in the region of the focal maximum on the axis of a diagnostic transducer even with the formation of a developed shock in the wave profile at the focus, with the error of calculation being 15%. The boundary conditions in the KZK equation should be such that the linear distribution of the pressure amplitude on the transducer axis in the region of the focal peak is as close as possible to the structure of the real field.

ACKNOWLEDGMENTS

REFERENCES

1. Shah, A., Owen, N., Lu, W., et al., *Urol. Res.*, 2010, vol. 38, no. 6, p. 491.
2. Harper, J.D., Cunitz, B.W., Dunmire, B., et al., *J. Urol.*, 2016, vol. 195, no. 4, p. 956.
3. Sarvazyan, A.P., Rudenko, O.V., and Nyborg, W.L., *Ultrasound Med. Biol.*, 2010, vol. 36, no. 9, p. 1379.
4. Doherty, J.R., Trahey, G.E., Nightingale, K.R., et al., *IEEE Trans. Ultrason., Ferroelectr., Freq. Control*, 2014, vol. 60, no. 4, p. 685.
5. Westervelt, P.J., *J. Acoust. Soc. Am.*, 1963, vol. 35, no. 4, p. 535.
6. Yuldashev, P.V. and Khokhlova, V.A., *Acoust. Phys.*, 2011, vol. 57, no. 3, p. 334.
7. Kurganov, A.R. and Tadmor, E., *J. Comput. Phys.*, 2000, vol. 160, p. 241.
8. Zabolotskaya, E.A. and Khokhlov, R.V., *Sov. Phys. Acoust.*, 1969, vol. 15, p. 35.
9. Karzova, M., Cunitz, B., Yuldashev, P., et al., *AIP Conf. Proc.*, 2016, vol. 1685, p. 040002.
10. Rosnitskiy, P.B., Yuldashev, P.V., and Khokhlova, V.A., *Acoust. Phys.*, 2015, vol. 61, no. 3, p. 301.
11. Tjotta, J.N., Tjotta, S., and Vefring, E.H., *J. Acoust. Soc. Am.*, 1991, vol. 89, no. 3, p. 1017.
12. Hamilton, M.F., Rudenko, O.V., and Khokhlova, V.A., *Acoust. Phys.*, 1997, vol. 43, no. 1, p. 39.
13. Canney, M.S., Bailey, M.R., Crum, L.A., et al., *J. Acoust. Soc. Am.*, 2008, vol. 124, p. 2406.
14. Perez, C., Chen, H., Matula, T.J., et al., *J. Acoust. Soc. Am.*, 2013, vol. 134, no. 2.
15. Rosnitskiy, P.B., Yuldashev, P.V., Vysokanov, B.A., and Khokhlova, V.A., *Acoust. Phys.*, 2016, vol. 62, no. 2, p. 151.
16. Rosnitskiy, P.B., Yuldashev, P.V., Sapozhnikov, O.A., Maxwell, A.D., Kreider, W., Bailey, M.R., and Khokhlova, V.A., *IEEE Trans. Ultrason., Ferroelectr., Freq. Control*, 2017, vol. 64, no. 2, p. 374.
17. Gavrilov, L.R., Sapozhnikov, O.A., and Khokhlova, V.A., *Bull. Russ. Acad. Sci.: Phys.*, 2015, vol. 79, no. 10, p. 1232.
18. Bessonova, O.V., Khokhlova, V.A., Bailey, M.R., Canney, M.S., and Crum, L.A., *Acoust. Phys.*, 2009, vol. 55, nos. 4–5, p. 463.

CONCLUSIONS

We found that the axially symmetric parabolic Khokhlov–Zabolotskaya–Kuznetsov equation can be

Translated by E. Berezhnaya